Ad Hoc Networks 122 (2021) 102628

Contents lists available at ScienceDirect

Ad Hoc Networks

journal homepage: www.elsevier.com/locate/adhoc

Travel Hopping Enabled Resource Allocation (THEResA) and delay tolerant networking through the use of UAVs in railroad networks

Elias Yaacoub

Department of Computer Science and Engineering, Qatar University, P.O. Box 2713, Doha, Qatar

ARTICLE INFO

Keywords:
Railroad networks
UAV
6G
Delay tolerant networks
Beamforming

ABSTRACT

This paper investigates the use of unmanned aerial vehicles (UAVs)/drones for providing high data rates to mobile relays (MRs) placed on top of high speed train wagons, thus introducing the concept of Travel Hopping Enabled Resource Allocation (THEResA). The objective is to provide high data rate connectivity to train passengers in 5G+/6G networks. With the drone flying at the same train speed, highly directive beams can be formed and steered between the drone and each of the MRs. The simulation results in the paper show that this leads to high data rate connectivity, which will be reflected in the indoor links between the MRs and the train passengers inside the wagons. The drones maintain the connectivity to the cellular infrastructure by using high speed links with the cellular base stations (BSs) deployed along the rail track, e.g., through free space optics (FSO). The drones use the BS sites for recharging and resuming their operation. Therefore, a separate set of drones, or the same drones when they are not flying over trains, can be used to provide connectivity to remote rural areas. In fact, high speed trains might travel through rural areas with low population density. Although it is practical to lay fiber optic cables along the rail track, villages and small rural population agglomerations far from the railroad might not have access to the internet backhaul. UAVs can provide this connectivity in a delay tolerant fashion, by heading from the BSs/train station sites towards remote areas, collecting/transferring data from/to these areas, then returning to the sites along the rail track to recharge their batteries. This paper presents an analysis that shows the feasibility of this approach.

1. Introduction

With the advances in 5G and beyond cellular networks, users are expecting ubiquitous connectivity at increasingly higher data rates and enhanced quality of service/quality of experience (QoS/QoE). Passengers in high speed trains are no exception, although providing them with the same levels of QoE is relatively challenging. Connectivity in high speed trains has been investigated in several works in the literature, e.g., [1–8]. In [1–3], remote radio heads (RRHs) and/or small cells are considered to be deployed along the rail track, in order to provide connectivity by communicating with a mobile relay (MR) located on top of the train. The short range RRH-MR connectivity can be performed over millimeter wave (mmWave) communications [1,4]. One MR was considered in [1], whereas two MRs (front and rear) were assumed in [2], and several ones were considered in [3]. The presence of MRs allows generally line of sight (LOS) communication with the base stations (BSs) deployed along the rail track, and due to their wired connection with the internal train network, they allow avoiding the penetration loss that is inevitable when radio signals have to propagate directly from the outdoor BSs to the user equipment (UEs) inside the train wagons. The presence of frequent RRHs along the track would lead to several handovers. Therefore, it would be good to benefit from the capabilities of MRs, e.g., to be equipped with massive multiple-input multiple-output (MIMO) antennas or to support intelligent radio resource management (RRM), in order to provide backhaul connectivity to the BSs along the rail track while avoiding excessive handovers at high speed with RRHs deployed along the track with shorter distances between them [5,6]. Some works have also considered the train control data traffic, which can be transmitted over a separate network or over the same network as the passenger data [7]. In fact, with 5G and beyond network deployments along with software defined networking and network function virtualization, the concept of network slicing has emerged. Thus, a slice dedicated for 5G massive machine type communications (mMTC) can be used for the transmission of train control and management system (TCMS) data without disrupting the passenger data [8].

Several other papers in the literature have addressed the problem of connectivity for high speed trains. The brief overview in this section has discussed the most relevant ones that mostly focus on using the more recent 5G communications. Most of the papers in the literature consider

E-mail address: eliasy@ieee.org.

https://doi.org/10.1016/j.adhoc.2021.102628
Received 24 March 2021; Received in revised form 7 June 2021; Accepted 19 July 2021
Available online 27 July 2021

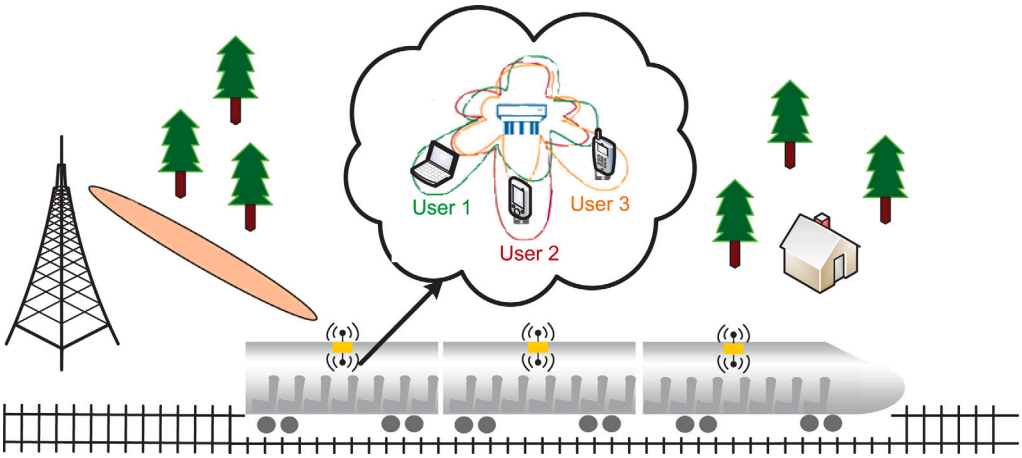

Fig. 1. Railroad example with MRs.

MRs and/or antennas on top of train wagons from the perspective of ensuring connectivity and handover efficiency. In addition, relatively few papers (e.g., [5,6]) investigate RRM with MRs. However, most papers do not consider the use of massive adaptive antenna arrays in conjunction with smart RRM for the purpose of increasing the data rates and the QoS for passengers traveling at high speed inside the train with 5G/5G+ networks.

On the other hand, unmanned aerial vehicles (UAVs) have been used recently to fly over rail networks, mainly for the purpose of monitoring the state of the tracks, detecting faults or any problematic issues, in order to enhance maintenance and prevent any accidents [9, 10]. Moreover, UAVs/Drones have been used to provide backhaul connectivity, or to act as flying BSs, in order to allow users in remote and rural areas to access the internet [11–13]. However, according to the author's knowledge, they have not been used to enhance the connectivity for train passengers.

Therefore, this paper investigates the use of drones equipped with adaptive antenna arrays to provide high speed data rates to train passengers through the MRs placed on top of train wagons in a Travel Hopping Enabled Resource Allocation (THEResA) approach. Since the speed of drones is becoming comparable to that of high speed trains (in the order of 250 km/h) [14,15], this option becomes worthy of further investigation.

In addition, several works in the literature have studied the use of drones for providing connectivity to rural areas, where a permanent backhaul infrastructure is hard to deploy. For example, in [12,13], a UAV is used to hover over a certain rural area, and act as a 5G BS providing coverage to that area. The UAV is connected to the backbone network through a number of limited fixed BS sites where fiber optic connections are provided in order to connect these BS sites to each other and to the core network. These sites serve for recharging the battery-operated UAVs while other UAVs are hovering over the region. Consequently, a group of UAVs provides 5G connectivity while another group is recharging, and then they switch roles, and so on. This approach was shown to be more economical than relying on a full network of ground BSs to cover the remote rural area. The economical feasibility of this approach was studied in [16]. It was shown that in the absence of government support/subsidies, subscription fees of around 20 Euros/month would make such a deployment viable in certain rural areas. The minimization of the drones' energy consumption while providing adequate cellular coverage in rural areas was investigated in [17], and a solution based on Genetic Algorithms is proposed. As in [12,13], the scenario of [17] assumes that UAVs recharge their batteries at certain ground sites then fly to their allocated zones to provide 5G coverage. A similar concept can be implemented in the railroad scenario, where the charging stations can be placed at the BS sites along the track or within the train stations at specific locations. This paper addresses this scenario, where the UAVs can travel to the remote areas whenever possible and provide intermittent connectivity in a delay tolerant networking (DTN) fashion.

Hence, the main contributions of the paper can be summarized as follows:

- Using UAVs to travel above the train at the same speed in conjunction with MRs placed on top of train wagons, in order to overcome the limitations of a direct connection between the MRs and cellular BSs deployed along the track.
- Performing highly directive beamforming between antennas placed at the UAV and at the MRs in order to provide high data rates to the train passengers.
- Using UAVs that can be recharged at the train stations, in order to provide connectivity in a DTN fashion to remote isolated villages in remote rural areas. The proposed scenario is formulated as a traveling salesman problem (TSP) and a heuristic nearest neighbor solution is studied, taking into account the limitations of the UAVs.

The rest of this paper is organized as follows. The problem statement and system model are provided in Section 2. The proposed approach is presented in Section 3. In Section 4, simulation results are presented, analyzed, and discussed. The DTN approach using UAVs flying from train stations is described and analyzed in Section 5. Finally, conclusions are drawn in Section 6.

2. Problem statement and system model

This section describes the problem investigated in this paper, and presents the system model used in the proposed approach. We investigate a railway scenario where MRs are deployed on top of train wagons. They have outdoor antennas that allow them to communicate with the BSs deployed along the rail track. In addition, they have other indoor antennas that allow them to communicate over a local area network (LAN) inside each wagon. For example, this could be through a WiFi network, or through LTE-Advanced (LTE-A) indoor femtocells. Fig. 1 shows this scenario, where the MRs can also perform user specific beamforming to further boost the indoor data rates.

However, this approach has a limitation on the outdoor part when BSs need to perform adaptive beamforming towards the MRs. In fact, Fig. 2 shows the elevation angles at the different MRs for BS and train antennas in a scenario with 10 MRs, and how they change along the rail track from a distance of 100 m up to 2500 m from the BS. Clearly, the beams destined for the various MRs will significantly overlap as the train moves away from the BS. Even at a close distance of 100 m, the difference between the first and last MR does not exceed eight

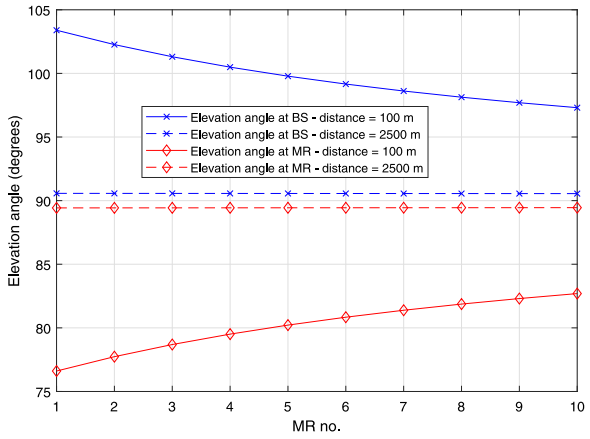

Fig. 2. Elevation angles at the different mobile relays for BS and train antennas.

degrees, still indicating that it will be hard to separate the beams steered towards consecutive MRs.

Therefore, to provide beamforming towards the MRs while avoiding significant overlap of the steered beams, we investigate the use of drones to provide connectivity to the MRs. The drones will travel above the train at the same speed while performing beamforming towards the train's MRs, thus implementing travel hopping resource allocation (THEResA), as shown in Fig. 3. More details about this scenario are presented in Section 3.

3. Proposed approach

The proposed approach in this paper is based on using drones equipped with adaptive antenna arrays to provide high speed data rates to train passengers through the MRs placed on top of train wagons. Since the speed of drones is becoming comparable to that of high speed trains (in the order of 250 km/h) [14,15], the drone can fly over the train at the same speed during its trajectory between two or more BSs. The investigated scenario is shown in Fig. 3. Thus, the UAV/drone will act as a sort of relay between the MRs and the BS, or even can be considered as a sort of "flying RRH". Since in open areas with high speed trains a line of sight is generally available in the scenario of Fig. 3 where BSs are deployed along the rail track, the drone can communicate with the BS using free space optics (FSO) for example. High speed communication between ground stations and UAVs moving at high speed has been demonstrated, e.g., see [18].

In the scenario of Fig. 3, the drone can be connected to one or two BSs along the rail track, such that the communication with the MRs can be handed over to the next BS as the train becomes closer to it. The drone can continue flying until it needs recharging, where another drone can replace it by flying over the train (since the train trajectory is know, its arrival time can be estimated and the drone can fly early enough to reach the required speed when the train arrives). In practice, if a train is moving at a speed of v_{train}, and the drone needs t_S seconds to reach this speed, then it should be launched when the train is still at a distance of $d = v_{\text{train}} \cdot t_S$ from the launch site, so that the drone can smoothly fly over the train at the same speed. Moreover, it can be maintained at a fixed altitude using positioning sensors at the wagons and the drone. The altitude is selected in order to allow sufficient separation between the antenna beams, thus avoiding the scenario of Fig. 2. Naturally, this altitude can be maintained as long as the terrain conditions allow (which should be feasible across long stretches of rail tracks in rural areas for example). When the train enters a tunnel for example, the drone has to fly above it and the connection with the train will be lost. This can be compensated for by having a BS at the tunnel entrance with several RRHs connected to it and positioned appropriately inside the tunnel. Recharging of the drones can take place at the BS sites. Thus, after recharging, the drone can return to its original base by flying over another train heading in the opposite direction. The design of the network, including the number of flying versus recharging drones, the recharging sites at BS locations, etc., can be performed based on the rail traffic in the area considered.

Table 1
Definitions.

Variable	Description
$P_{\text{T,i}}$	Power of signal from UAV towards MR i.
$H_{\text{T,i}}$	Channel gain between the UAV and MR i.
$G_{\text{T,i}}$	Gain of the antenna array of the UAV with its main beam steered in the direction of MR i (θ_i, ϕ_i)
$G_{\text{i,T}}$	Gain of the antenna of MR i in the direction of the UAV (θ_T, ϕ_T)
σ^2	Noise power
I_{i}	Total interference power received at MR i
$\text{SINR}_{T,i}$	Signal to Interference plus Noise Ratio on the link between the UAV and MR i
$C_{T,i}$	Channel capacity of the link between the UAV and MR i
$d_{T,i}$	Distance between the UAV and MR i
$F_{T,i}$	Fast fading on the link between the UAV and MR i
$\psi_{T,i}$	Log-normal shadowing on the link between the UAV and MR i

3.1. Channel model

The wireless channel model between the UAV and MR i is characterized by the following channel gain equation [19]:

$$H_{T,i,\text{dB}} = (\kappa - 10\gamma \log_{10} d_{T,i}) + \psi_{T,i} + 10 \log_{10} F_{T,i} \quad (1)$$

where κ is the pathloss constant, $d_{T,i}$ is the distance between the drone and MR i, γ is the path loss exponent, $\psi_{T,i}$ represents log-normal shadowing with zero mean and a standard deviation σ_ψ, and $F_{T,i}$ corresponds to fast fading assumed to be averaged out by adaptive modulation and coding and thus not considered in the results of the UAV–MR links in this paper, especially with the dominance of the line of sight component in the channel model.

3.2. SINR calculations

The Signal to Interference plus Noise Ratio (SINR) on the link between the UAV and MR i is given by (2), where the parameters used are defined in Table 1. The downlink direction is considered where the UAV is the transmitter (thus denoted by the subscript T in the equations).

$$\text{SINR} = \frac{P_{\text{T,i}} H_{\text{T,i}} G_{\text{T,i}}(\theta_i, \phi_i) G_{\text{i,T}}(\theta_T, \phi_T)}{I_{\text{i}} + \sigma^2} \quad (2)$$

In (2), I_{i} is the total interference power received at MR i, due to the transmissions to other MRs in case they are allocated the same frequency. It is given by:

$$I_{\text{i}} = \sum_{j=1; j \neq i}^{K} \delta_{ij} P_{\text{T,j}} H_{\text{T,i}} G_{\text{T,j}}(\theta_i, \phi_i) G_{\text{i,T}}(\theta_T, \phi_T) \quad (3)$$

In (3), K is the number of MRs, and δ_{ij} is an indicator variable; it is set to 1 if MRs i and j are allocated the same frequency channel in Fig. 3, and set to 0 otherwise. In addition, $G_{\text{T,j}}(\theta_i, \phi_i)$ indicates the antenna gain in the direction of MR i, (θ_i, ϕ_i), when the main beam is steered in the direction of MR j. It corresponds to the power that leaks towards undesired directions (in this case that of MR i), from the signal directed towards MR j.

In Section 4, we present results where the MRs are equipped either with omnidirectional antennas, or with massive MIMO arrays. When a single omni-directional antenna is used by each MR, $G_{\text{i,T}}$ is set to one in all directions for all MRs i in (2) and (3). When an antenna array is used at each MR, we consider the same array type used at the

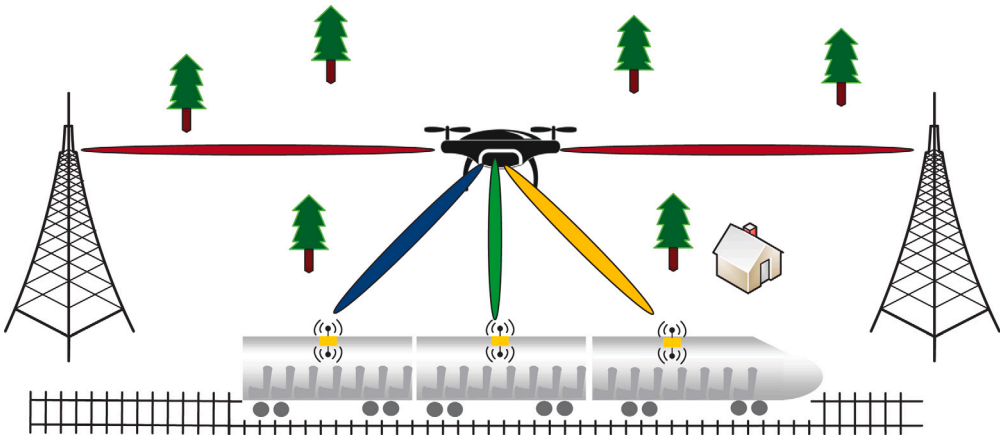

Fig. 3. Railroad scenario with MRs connected to a drone.

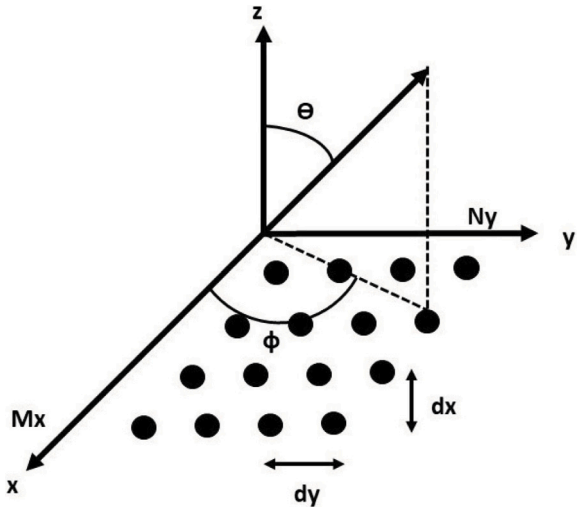

Fig. 4. Planar antenna array in the x–y plane.

UAV (although different types can be used in practice if needed). The design of the antenna arrays is discussed in Section 3.4, where multiple configurations are described and their performance is compared in Section 4.

3.3. Capacity calculation

The objective is to maximize the SINR of each MR (in order to serve the users inside their respective wagons at high data rates), thus maximizing their channel capacity given by:

$$C_{T,i} = B \cdot \log_2(1 + \text{SINR}_{T,i}) \tag{4}$$

where $C_{T,i}$ and $\text{SINR}_{T,i}$ are the channel capacity and SINR, respectively, on the link between the UAV and MR i ($i \in \{1, \ldots, K\}$, assuming we have K = MRs, and B is the channel bandwidth.

3.4. Antenna design

This section describes the antenna arrays used in the simulations of this paper. We consider that the UAV has a massive planar antenna array placed at its lower side facing the train MRs, with M antenna elements spaced by d_x in the x-direction and N elements spaced by d_y in the y-direction. In fact, planar antenna arrays consist of antenna elements positioned along a rectangular grid [20], as shown in Fig. 4 (for the array at the UAV, the z-axis should be pointing downwards to correspond to the scenario of Fig. 3; however, it is shown pointing upwards in Fig. 4 for clarity purposes).

Such an array consists of linear arrays on the x-axis, with a progressive phase shift β_x between the elements on the x-axis. The array factor of one of these linear arrays is given by [20]:

$$\text{AF}_{\text{linear,x}}(\theta, \phi) = \sum_{m=1}^{M} I_m e^{j(m-1)(kd_x \sin\theta\cos\phi + \beta_x)} \tag{5}$$

where I_m is the excitation coefficient of each element, and k is the wave number.

Similarly, the planar array consists of linear arrays on the y-axis, with a progressive phase shift β_y between the elements on the y-axis. The array factor of one of these linear arrays is given by [20]:

$$\text{AF}_{\text{linear,y}}(\theta) = \sum_{n=1}^{N} I_n e^{j(n-1)(kd_y \sin\theta\sin\phi + \beta_y)} \tag{6}$$

where I_n is the excitation coefficient of each element.

It can be shown that the array factor of the planar array is equal to the multiplication of the array factor of a linear array on the x-axis by that the array factor of a linear array on the y-axis [20]:

$$\text{AF}_{\text{planar}}(\theta, \phi) = \text{AF}_{\text{linear,x}}(\theta, \phi) \times \text{AF}_{\text{linear,y}}(\theta, \phi) \tag{7}$$

$$\text{AF}(\theta, \phi) = \sum_{n=1}^{N} I_n \left[\sum_{m=1}^{M} I_m e^{j(m-1)(kd_x \sin\theta\cos\phi + \beta_x)} \right] e^{j(n-1)(kd_y \sin\theta\sin\phi + \beta_y)} \tag{8}$$

In order to steer the main-lobe to a certain desired direction (θ_o, ϕ_o), the progressive phase shifts β_x and β_y must satisfy:

$$\beta_x = -kd_x \sin\theta_o \cos\phi_o \tag{9}$$

$$\beta_y = -kd_y \sin\theta_o \sin\phi_o \tag{10}$$

In the proposed approach, since the MR is moving at the same speed of the train, the beams are formed once and do not have to be continuously steered, since the UAV and MRs appear to be fixed with respect to each other.

The antenna gain is generally calculated from the antenna directivity, after multiplying it by a certain loss factor that has generally a value close to one [20]. The directivity in the direction (θ_o, ϕ_o) is calculated from the array factor $\text{AF}(\theta, \phi)$ as follows [20]:

$$\text{D}(\theta_o, \phi_o) = 4\pi \frac{|\, AF(\theta_o, \phi_o)\,|^2}{\int_0^{2\pi}\int_0^{\pi} |\, AF(\theta, \phi)\,|^2 \sin\theta d\theta d\phi} \tag{11}$$

The above expression calculates the directivity in the direction of maximum radiation (θ_o, ϕ_o), which we consider equal to the antenna gain in that direction. The gain in any other direction (θ_j, ϕ_j) can be calculated by replacing (θ_o, ϕ_o) with (θ_j, ϕ_j) in (11).

Table 2
Simulation parameters for the outdoor scenario.

Variable	Description
κ	−38.89 dB
γ	2.05
σ_w	3.8 dB
Separation between MRs on neighboring wagons	10 m
Separation between BSs (inter-BS distance)	5 km
Number of wagons in the train	10
Wagon length	10 m per wagon
Train speed	250 km/h
UAV transmit power	5 W
UAV Height above ground	48 m
MR Height above ground	3 m
Duration of one transmission time interval (TTI)	1 ms
Available bandwidth	100 MHz
Receiver noise power σ^2	−196.97 dBW/Hz

In this paper, we investigate different array types characterized by various methods for setting their excitation coefficients I_m and I_n. We consider different methods for setting these values for linear arrays, such that the excitation of an element at position (m, n) in the planar array will be $I_{m,n} = I_m \times I_n$.

The simplest approach is to consider uniform excitation, where in a linear array we would have $I_m = 1$ for all m. Chebyshev arrays are another type of linear arrays. They have the unique property that all side lobes in their radiation pattern are of equal magnitude. The excitation currents of the elements of a Chebyshev array are related to the coefficients of a Chebyshev polynomial [20,21]. In [22], another current distribution is presented where the excitation coefficients are those of a Kaiser window. It is called the Bessel current distribution. It has the property that a maximum sidelobe level can be defined, such as the other sidelobe levels have decreasing magnitudes. However, this comes at the expense of a wider main beam compared to Chebyshev excitation.

In this paper, we consider various combinations of these excitations in the investigated planar arrays. For example, we consider uniform excitation for the elements along the x-axis, with uniform, Chebyshev, or Bessel excitation of the elements on the y-axis. Then, we investigate the Chebyshev excitation for the elements along the x-axis, with uniform, Chebyshev, or Bessel excitation of the elements on the y-axis. Finally, we study the Bessel excitation for the elements along the x-axis, with uniform, Chebyshev, or Bessel excitation of the elements on the y-axis.

4. Results and discussion

This section presents the simulation results by using the proposed THEResA approach of Section 3.

4.1. Simulation parameters

The simulation parameters are shown in Table 2. In (1), the parameters are set according to [23,24]. We assume that the antenna array at the bottom of the drone has 10×10 antenna elements separated by $d_x = d_y = 0.5\lambda$ (where λ is the wavelength). The antenna excitation coefficients are calculated according to the techniques in [20,22] such that the side lobe levels with Chebyshev arrays and the maximum side lobe level with Bessel arrays are set to 20 dB below the main beam. We track the data rate achieved by each of the MRs along with the various antenna configurations at the UAV and MRs.

Two main scenarios are considered:

- No interference scenario: The bandwidth is subdivided equally among the MRs, such that there is no interference from the signals destined to one MR on the other MRs. This leads to setting the interference terms in I_i in (2) and (3) to zero. However, each MR gets a bandwidth of 10 MHz.

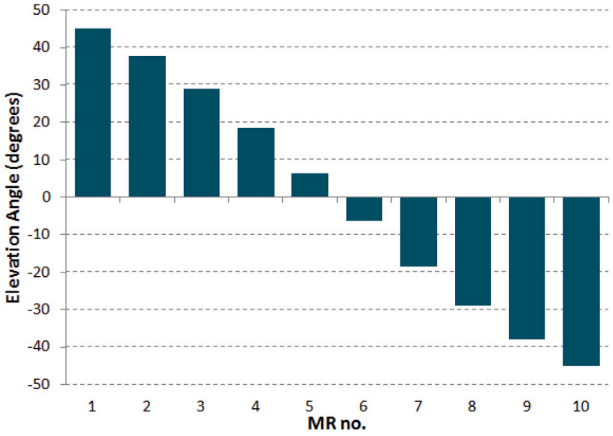

Fig. 5. Elevation angles at the different mobile relays between the UAV and train antennas.

- Interference scenario: The whole 100 MHz bandwidth is allocated to each MR. Thus, we rely on space division multiple access (SDMA) through the beamforming approach of Fig. 3. However, since practical antennas are used, they have non-negligible power radiated through the sidelobes. This will cause interference from the signals destined to one MR to the other MRs, and the interference terms I_i will be calculated according to (3) and used in (2).

4.2. Simulation results

Fig. 5 shows the elevation angles between the drone and each of the MRs with the proposed THEResA approach. There is at least a difference of eight degrees in elevation between consecutive MRs (and this difference remains constant throughout the trajectory due to the presence of the drone), which provides a clear advantage over the scenario of Fig. 2, where at even the best scenario the first and last MRs were separated by eight degrees (i.e., less than one degree separation between consecutive MRs).

Figs. 6 and 7 show the data rates achieved by each antenna type, averaged over fading realizations and summed for all MRs, for the interference and no interference scenarios, respectively. Clearly, the no interference scenario achieves significantly better results. In the absence of interference, the various antenna arrays have a comparable performance, as seen in Fig. 7. In the interference scenario, the results of Fig. 6 show that the arrays with uniform excitation along the x-axis (direction parallel to the train) have the best performance. This is due to their narrower main beam and thus relatively higher gain. Moreover, although their first sidelobe level is around 13 dB below the main beam, compared to 20 dB in the other arrays, they have lower levels in the other sidelobes. These results are achieved regardless of the distance between the train and the nearest BS, due to the presence of the UAV above the train.

Fig. 7 shows results where the beamforming is performed at both the UAV and the MRs (using planar arrays), or where it is performed only at the UAV (assuming MRs have omnidirectional antennas). It should be noted that both scenarios lead to the same result in the case of interference, since the antenna gain at the MR will amplify both the useful and interfering signal in its direction. Therefore, one set of results is shown in Fig. 6 to represent both cases.

To compare these results to the scenario without UAV, Fig. 8 shows the data rate versus the distance to the BS at the first MR (closest MR to the BS), when all the wireless channels are allocated to it without any interference (in order to maximize performance, since it suffers the least attenuation due to being closer to the BS). The results fluctuate with the

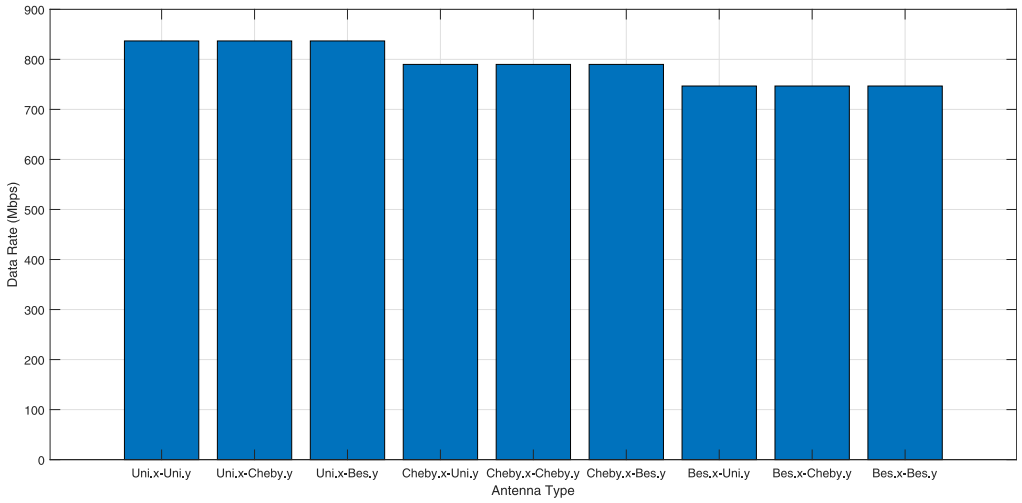

Fig. 6. Data rates achieved by each antenna type, averaged over all MRs, in the interference scenario.

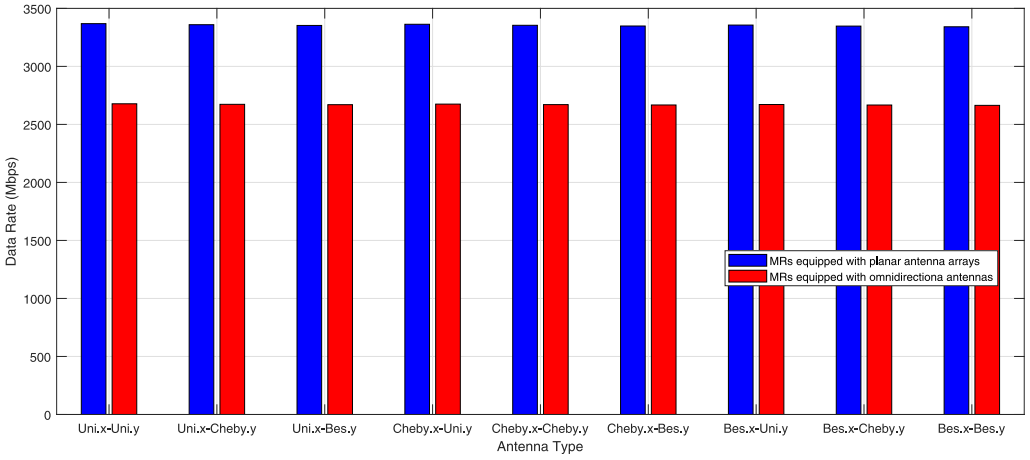

Fig. 7. Data rates achieved by each antenna type, averaged over all MRs, in the no interference scenario.

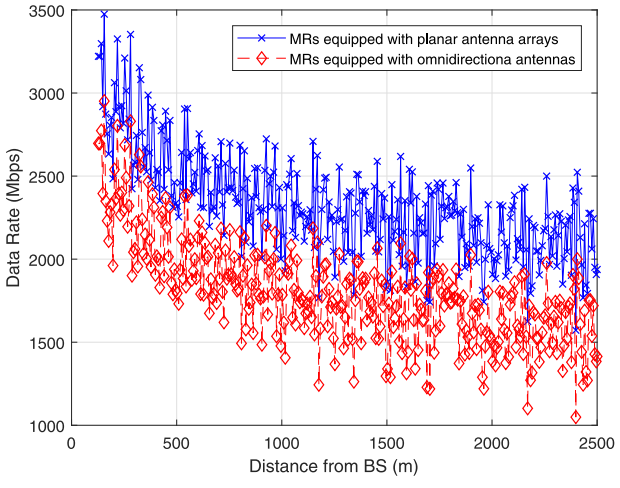

Fig. 8. Data rate versus distance achieved by MR no. 1.

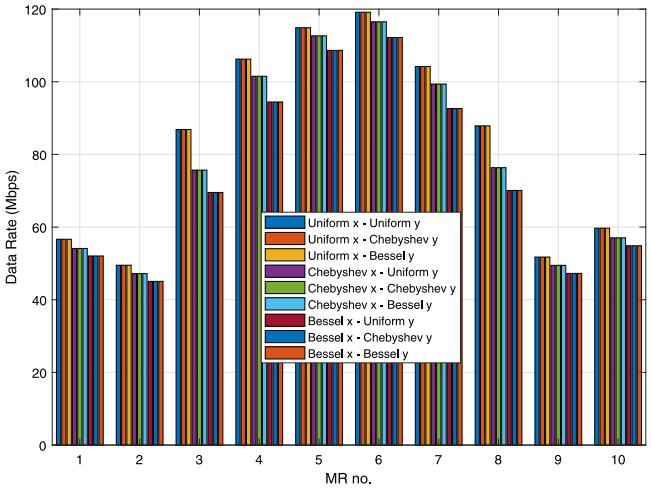

Fig. 9. Data rates achieved by each MR in the interference scenario.

fading realizations, but decrease significantly with the distance to the nearest BS, starting from 3 Gbps and 2.5 Gbps average data rates for the scenarios with beamforming performed at both the BS and the MR, or only at the BS, respectively. In the UAV case, the values of 3.3 Gbps and 2.7 Gbps shown in Fig. 7 for these respective cases are maintained irrespective of the distance to the BS, due to the presence of the UAV.

Figs. 9 and 10 show the data rates achieved by each MR for each antenna type, for the interference and no interference scenarios (with

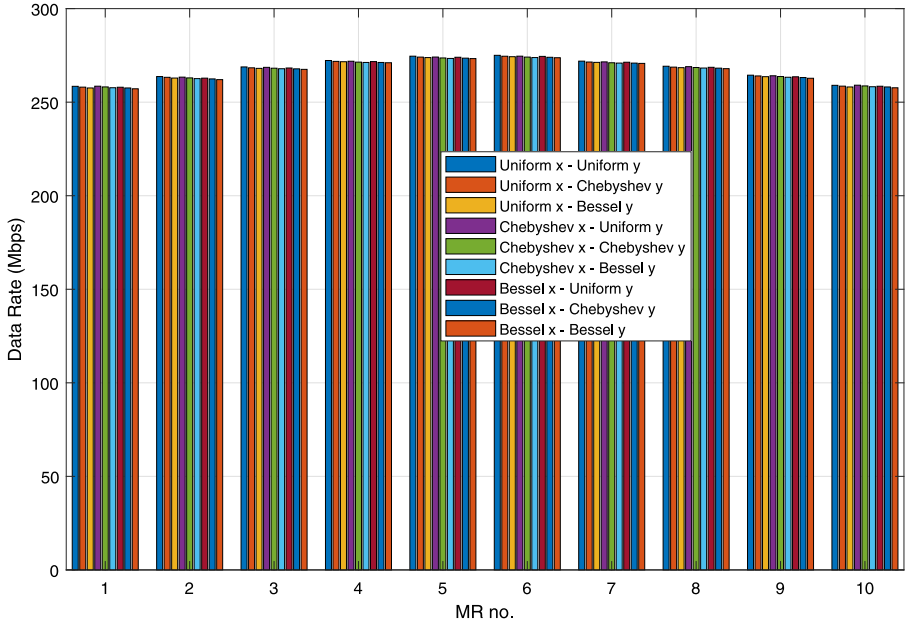

Fig. 10. Data rates achieved by each MR in the no interference scenario.

omnidirectional antennas at the MRs), respectively. As noted previously, the no interference scenario achieves significantly better results. In addition, as expected, the data rate will decrease with distance, i.e., the data rates decrease when the MR is located further away from the drone. Interestingly, in the no interference scenario, the decrease with distance is negligible within the dimensions considered in this numerical example.

The results of Fig. 10 show a total sum-rate in the order of 2.5 Gbps, which is within the range achievable by a typical FSO link [25–28]. In other words, the UAV-BS link can support the data rates at the UAV–MR links. Consequently, the UAV can maintain this high data rate backhaul connectivity between the MRs and the BS, thus allowing the MRs to successfully serve the indoor train passengers.

5. DTN coverage in rural areas

This section describes the use of drones to provide network coverage to rural areas, by benefiting from the railroad infrastructure for recharging, connecting to the core network, and maintenance.

In fact, the drones can benefit from connectivity to the core network through the BSs and fiber optic links reaching the train stations, in order to periodically and regularly hover over remote areas and provide them with internet connectivity thus implementing delay tolerant networking (DTN), as illustrated in Fig. 11. This is an important difference with [12,13,16,17] where the drones are assumed to be continuously above the covered areas and act as 5G BSs. Our motivation is different in the sense that the investigated scenario in this paper assumes the areas are too remote (otherwise they can be connected directly to the telecommunication infrastructure that would typically accompany the railroad), and providing them with permanent connectivity is too costly. The presence of the railway helps by placing the drones within feasible travel distance from these remote agglomerations, and the drones can provide intermittent DTN connectivity, with the charging-hovering cycles planned according to the capabilities of the drones, the location of the remote areas, and the availability of BS sites or train stations along the rail track.

This approach can be used not only to provide connectivity to remote households in rural areas, but also to provide connectivity for sensor networks and internet of things (IoT) devices deployed in these areas. For example, in [29], UAVs are used to gather the measurements of IoT sensors deployed in rural areas for farming applications. The

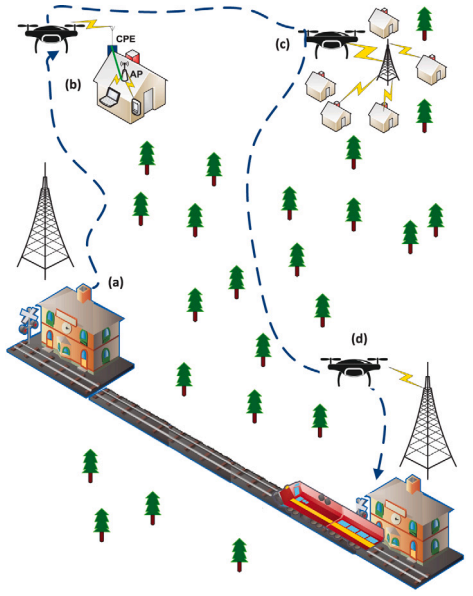

Fig. 11. DTN scenario with drones benefiting from the railroad network.

UAVs would hover over the deployment area, and carry the measurements back to a 5G BS, where the UAVs can be recharged when needed. Moreover, to avoid excessive delays in sending and analyzing the data, the BS site can be equipped with edge computing servers. Hence, the measurements can be processed and analyzed for the target farming application in the absence of connectivity to cloud servers.

5.1. Calculation of the flying time

We consider that a UAV, recharged at the train station, leaves to provide DTN coverage for n rural areas, before returning to the train station for recharging. This latter station could be the one that the UAV started from or a different one. The UAV can then return to the initial station later (i) by going through the trajectory in reverse (from region n to region 1), (ii) by going through a different trajectory,

e.g., providing connectivity through DTN to a group of villages/remote zones in another direction from the railway, (iii) by hovering over a train as discussed in Section 3 to return from the end station to the starting station, (iv) or even by being carried by a train as it travels between stations, where it can be offloaded when the train stops at the desired station (it can continue to be recharged on board the train).

The time needed to travel from the train station to the first coverage area is denoted by:

$$t_{\text{in}} = \frac{d_1}{v} \tag{12}$$

where d_1 is the distance between the station and the first area and v is the speed of the drone/UAV.

Similarly, the time needed to travel from the last (nth) coverage area to the train station is denoted by:

$$t_{\text{out}} = \frac{d_n}{v} \tag{13}$$

where d_n is the distance between the last covered area and the destination station.

Moreover, the time to travel between two consecutive areas i and $i+1$ separated by a distance $d_{i,i+1}$ would be:

$$t_{i,i+1} = \frac{d_{i,i+1}}{v} \tag{14}$$

The hovering time over coverage area i is denoted by:

$$t_{\text{hover},i} = \frac{S_i}{R_i} \tag{15}$$

where S_i is the total data (in bits) to be transferred from location i and R_i is the average transfer data rate achievable by the drone while hovering over area i. In (15), we assume that in area i, the drone can either:

- Get the data from a local access point (AP), such that the subscribers in that area communicate with the AP locally, and the UAV collects the data from the AP at specific time intervals (and also delivers to the AP any data destined to the subscribers in that area).
- Or, get the data directly from the subscribers, in case their homes are equipped with customer premises equipment, that can communicate with the drone similarly to the MRs of the train as in the scenario of Fig. 3 (of course, without the FSO connectivity in the DTN scenario). Beamforming and resource allocation can be performed by the drone to achieve data rates comparable to the results of Section 4. In this case, we assume that the houses/buildings are sufficiently close in the coverage area i such that the travel time within the area can be ignored; i.e., data transfer according to (15) is uninterrupted by travel times in area i (otherwise it can be split into multiple areas).

Fig. 11 illustrates both of these possibilities. In addition, similar assumptions can be made in the case of collecting IoT measurements, rather than providing connectivity to human subscribers: The drone can collect the data from a local AP/IoT controller that the sensors send their measurements to, or it can hover over a sensor deployment area (e.g., an agricultural field in an IoT farming application) to collect the sensor readings.

Thus, the total time per trip to provide coverage to the n areas and return is:

$$t_{\text{tot}} = t_{\text{in}} + t_{\text{hover},1} + \sum_{i=1}^{n-1}(t_{i,i+1} + t_{\text{hover},i+1}) + t_{\text{out}} \tag{16}$$

The expression in (16) can be simplified to:

$$t_{\text{tot}} = \sum_{i=0}^{n}(t_{i,i+1} + t_{\text{hover},i+1}) \tag{17}$$

where, in (17), it is assumed that $t_{0,1} = t_{\text{in}}$, $t_{n,n+1} = t_{\text{out}}$, and $t_{\text{hover},n+1} = 0$.

If the maximum energy that can be stored in the drone's battery after recharging is $E_{\max}$, and if P_f is the power consumed by the drone when flying, then the trajectory should be planned such that:

$$t_{\text{tot}} \leq \frac{E_{\max} - E_{\min}}{P_f} \tag{18}$$

where $E_{\min}$ is a residual energy used for safety measures, such that the trajectory planning is done in a way to avoid the drone battery energy going below $E_{\min}$. This allows to cater for unexpected conditions (reduced speed due to wind, more data to be collected than expected, etc.) without having the drone energy depleted or having to interrupt the mission in order to return for recharging.

When the starting and ending station are the same, the problem becomes similar to a traveling salesman problem (TSP): The drone has to visit each area to be served exactly once during a cycle, then return to the starting point to be recharged. This problem is known to be NP-hard [30,31]. Moreover, the trajectory planning should be performed such that (18) is satisfied. When the number of areas to be served from a given train station is limited, the brute-force optimal solution of the TSP problem can be obtained in reasonable time, and can be adopted if (18) is satisfied. If this is not the case, an approximation to the TSP solution can be used, e.g., the nearest neighbor approximation where the drone moves to the nearest unserved area as long as it can still return without violating (18). By denoting the maximum allowed energy cost ($E_{\max} - E_{\min}$) by $MaxCost$, and defining the energy cost to serve area i as $P_f \cdot (t_{i-1,i} + t_{\text{hover},i})$, then Algorithm 1 can be used to achieve this solution. This algorithm is implemented at each train station from which UAVs will take-off to serve remote areas. A UAV is added to the train station and starts visiting the remote areas one by one, until all areas are served or until reaching the limit set by (18). In this latter case, an additional UAV is added to the train station to serve the remaining areas, and so on until all areas are served.

Algorithm 1 Drone Trajectory Planning

```
while There are areas to be served using DTN do
    Add a drone to the zone controlled by the given train station
    TotalCost^(Old) = 0;
    TotalCost^(New) = TotalCost^(Old) + Cost to serve nearest area
    while (TotalCost^(New) + ReturnCost ≤ MaxCost) AND (There are still areas to be served) do
        TotalCost^(Old) = TotalCost^(New)
        Add the area to the route
        Remove the area from the set of areas to be served
        TotalCost^(New) = TotalCost^(Old) + Cost to serve nearest area
    end while
end while
```

A numerical example to provide better understanding of the order of magnitude of the above durations is given next in Section 5.2.

5.2. Numerical example

In the numerical example of this section, we consider a village located at a distance of 100 km from the railroad track, and where the data size that accumulates between drone visits is around 125 Gigabytes (equivalent to 1 terabits). A drone leaves the train station to provide connectivity to this area then returns for recharging its batteries. Hence, $n = 1$, $d_1 = d_n = 100$ km, and $S_1 = 10^{12}$ bits. We assume that the drone can travel at a speed of 250 km/h to reach the area (as per the assumptions of Sections 3 and 4) and can achieve a sum-rate of $R_1 = 2.5$ Gbps similarly to the simulation results of Section 4. Naturally, when hovering over the area, the drone would be moving at low speed while collecting the data, as opposed to the high travel speed when heading towards the coverage area. Using these numbers in Eq. (16) provides a total time of around 55 min. Thus, in

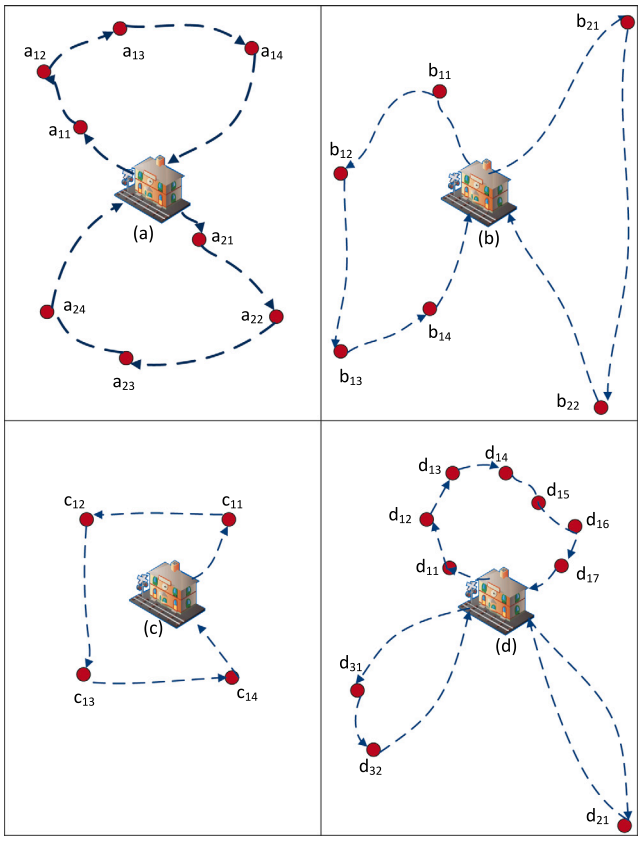

Fig. 12. DTN scenario with TSP implementation examples.

this example, the drone can travel to the remote area, collect/send the data using DTN, and return for recharging.

According to the numerical results of [17], a typical drone can spend an energy of around 200 Wh while on the move and recharge at the fixed site with an energy of 1000 Wh. Hence, the drone in the current example can visit three more villages (thus a total of four) with 100 km between them and then return to the railroad site (400 km trip) while still having 20% of stored energy to cater for unexpected conditions (reduced speed due to wind, longer than expected hovering time to collect extra data, etc.).

Fig. 12 shows additional examples corresponding to the implementation of Algorithm 1. In Fig. 12, we denote by x_{ij} the ith drone associated with train station x while serving the jth area allocated to it. Fig. 12(a) shows a scenario where two drones are needed to serve the remote areas around station (a): the first UAV serves the regions above the station whereas the second UAV serves the regions below the station. Fig. 12(b) shows another example where a UAV serves the regions to the left of train station (b) and another UAV serves the regions to its right. Fig. 12(c) shows an example where a single drone was sufficient to serve the remote areas around station (c). Finally, Fig. 12(d) shows a scenario where three UAVs are needed. In fact, due to having one very far location (d_{21}), a single drone is needed just to serve this area without exceeding the limit set by (18).

6. Conclusions

This paper investigated the use of UAVs/drones for providing high data rates to mobile relays placed on top of high speed train wagons. With the drone flying at the same train speed, highly directive beams can be formed and steered between the drone and each of the mobile relays. This was shown to provide high data rate connectivity, which will be reflected in the indoor links between the relays and the train passengers inside the wagons. The drones maintain the connectivity to the cellular infrastructure by using high speed links with the cellular BSs deployed along the rail track, e.g., through FSO. Moreover, since the drones use the BS sites for recharging and resuming their operation, they can be used to provide connectivity to remote rural areas when they are not flying over trains. In fact, high speed trains might travel through rural areas with low population density. Although it is practical to lay fiber optic cables along the rail track, villages and small rural population agglomerations far from the railroad might not have access to the internet backhaul. UAVs can provide this connectivity in a delay tolerant fashion, by heading from the BSs/train station sites towards remote areas, collecting/transferring data from/to these areas, then returning to the sites along the rail track to recharge their batteries. The analysis presented in this paper demonstrated the feasibility of this approach.

Declaration of competing interest

The authors declare that they have no known competing financial interests or personal relationships that could have appeared to influence the work reported in this paper.

Acknowledgments

The author would like to thank the Editor and the Anonymous Reviewers for their comments that helped in significantly enhancing the quality and clarity of this paper.

This publication was jointly supported by Qatar University and IS-Wireless - IRCC Grant no. IRCC-2021-003. The findings achieved herein are solely the responsibility of the author.

References

[1] L. Yan, X. Fang, H. Li, C. Li, An mmWave wireless communication and radar detection integrated network for railways, in: IEEE 83rd Vehicular Technology Conference (VTC Spring), 2016.

[2] J. Kim, et al., A comprehensive study on mmwave-based mobile hotspot network system for high-speed train communications, IEEE Trans. Veh. Technol. 68 (3) (2019).

[3] S. Banerjee, S.M. Rakshit, M. Hempel, H. Sharif, 5G-UCDA in high speed rail with multi antenna-to-logical cell circular FIFO mapping strategy, in: International Conference on Computing, Networking and Communications (ICNC), 2018.

[4] D. He, et al., Channel measurement, simulation, and analysis for high-speed railway communications in 5G millimeter-wave band, IEEE Trans. Intell. Transp. Syst. 19 (10) (2018) 3144–3158.

[5] H. Ghazzai, T. Bouchoucha, A. Alsharoa, E. Yaacoub, M.S. Alouini, T. Al-Naffouri, Transmit power minimization and base station planning for high-speed trains with multiple moving relays in OFDMA systems, IEEE Trans. Veh. Technol. 66 (1) (2017) 175–187.

[6] E. Yaacoub, R. Atat, A. Alsharoa, M.-S. Alouini, Mobile relays for enhanced broadband connectivity in high speed train systems, Phys. Commun. (Elsevier) 12 (2014) 105–115.

[7] A. Gonzalez-Plaza, et al., 5G communications in high speed and metropolitan railways, in: 11th European Conference on Antennas and Propagation (EUCAP), 2017.

[8] F. Hasegawa, et al., High-speed train communications standardization in 3GPP 5G NR, IEEE Commun. Stand. Mag. 2 (1) (2018) 44–52.

[9] THALES Group, How Drones will change the future of railways, 2019, url: https://www.thalesgroup.com/en/worldwide/transport/magazine/how-drones-will-change-future-railways [Accessed Feb. 25, 2021].

[10] Dart Drones, Drones for Railways: Real-world benefits, use cases and ROI, 2021, url: https://www.dartdrones.com/drones-for-railways/ [Accessed Feb. 25, 2021].

[11] E. Yaacoub, M.-S. Alouini, A key 6G challenge and opportunity—Connecting the base of the Pyramid: A survey on rural connectivity, Proc. IEEE 108 (4) (2020) 533–582.

[12] L. Chiaraviglio, L. Amorosi, N. Blefari-Melazzi, P. Dell'Olmo, C. Natalino, P. Monti, Optimal design of 5G networks in rural zones with UAVs, optical rings, solar panels and batteries, in: 20th International Conference on Transparent Optical Networks (ICTON), Bucharest, Romania, 2018.

[13] L. Amorosi, L. Chiaraviglio, F. D'Andreagiovanni, N. Blefari-Melazzi, Energy-efficient mission planning of UAVs for 5G coverage in rural zones, in: IEEE International Conference on Environmental Engineering, Milan, Italy, 2018.

[14] J. Feist, Best racing drones — need for speed in the sky, dronerush, 2021, url: https://dronerush.com/best-racing-drones-speed-agility-fpv-5971/ [Accessed June 6, 2021].
[15] B. Popper, New Drone Claims Guinness World Record with a Top Speed of 163 Mph, The Verge, 2017, url: https://www.theverge.com/2017/7/14/15967948/drone-racing-league-fastest-drone-racerx-guinness-world-record-163-mph [Accessed June 6, 2021].
[16] L. Chiaraviglio, W. Liu, J.A. Gutierrez, N. Blefari-Melazzi, Optimal pricing strategy for 5G in rural areas with unmanned aerial vehicles and large cells, in: 27th International Telecommunication Networks and Applications Conference (ITNAC), Melbourne, VIC, Australia, 2017.
[17] J.G. Jiménez, L. Chiaraviglio, L. Amorosi, N. Blefari-Melazzi, Multi-period mission planning of UAVs for 5G coverage in rural areas: a heuristic approach, in: 9th International Conference on the Network of the Future (NOF), Poznan, Poland, 2018.
[18] L. Li, R. Zhang, Z. Zhao, et al., High-capacity free-space optical communications between a ground transmitter and a ground receiver via a UAV using multiplexing of multiple orbital-angular-momentum beams, Sci. Rep. 7 (2017) 17427, http://dx.doi.org/10.1038/s41598-017-17580-y.
[19] A. Goldsmith, Wireless Communications, Cambridge University Press, New York, NY, USA, ISBN: 978-0-521-83716-3, 2005.
[20] C.A. Balanis, Antenna Theory, Analysis and Design, fourth ed., John Wiley and Sons, 2016.
[21] B.K. Lau, Y.H. Leung, A dolph-chebyshev approach to the synthesis of array patterns for uniform circular arrays, in: IEEE International Symposium on Circuits and Systems, Geneva, Switzerland, May 28-31, 2000.
[22] K.Y. Kabalan, A. El-Hajj, M. Al-Husseini, Bessel planar arrays, Radio Sci. 39 (2004) RS1005, http://dx.doi.org/10.1029/2003RS002872.
[23] N.F. Abdullah, A.A. Goulianos, T.H. Barratt, A.G.L. Freire, D.E. Berraki, S.M.D. Armour, A.R. Nix, M.A. Beach, Path-loss and throughput prediction of IEEE 802.11ad systems, in: IEEE 81st Vehicular Technology Conference (VTC Spring), Glasgow, UK, 2015.
[24] R. He, Z. Zhong, B. Ai, J. Ding, An empirical path loss model and fading analysis for high-speed railway viaduct scenarios, IEEE Antennas Wirel. Propag. Lett. 10 (2011) 808–812.
[25] A. Bahrami, A. Lord, T. Spiller, Quantum key distribution integration with optical dense wavelength division multiplexing: a review, IET Quantum Commun. 1 (1) (2020) 9–15.
[26] A. Malik, P. Singh, Free space optics: Current applications and future challenges, Int. J. Opt. 2015 (2015) 945483, 7 pages.
[27] M. Bilgi, M. Yuksel, Throughput characteristics of free-space-optical mobile ad hoc networks, in: International Conference on Modeling, Analysis and Simulation of Wireless and Mobile Systems (MSWiM, Bodrum, Turkey, 2010, pp. 170–177.
[28] CableFree, Free space optics (FSO), 2021, url: https://www.cablefree.net/cablefree-free-space-optics-fso [Accessed Feb. 25, 2021].
[29] G. Faraci, A. Raciti, S. Rizzo, G. Schembra, A 5G platform for unmanned aerial monitoring in rural areas: Design and performance issues, in: 4th IEEE Conference on Network Softwarization and Workshops (NetSoft), Montreal, QC, Canada, 2018.
[30] B. Korte, J. Vygen, The traveling salesman problem, in: Combinatorial Optimization - Theory and Algorithms, fourth ed., Springer, Berlin, Heidelberg, ISBN: 978-3-540-71844-4, 2008, CHapter 21.
[31] I.M. Ross, R.J. Proulx, M. Karpenko, Autonomous UAV sensor planning, scheduling and maneuvering: an obstacle engagement technique, in: 2019 American Control Conference (ACC), Philadelphia, PA, USA, 2019, pp. 65–70.

Elias Yaacoub received the B.E. degree in Electrical Engineering from the Lebanese University in 2002, the M.E. degree in Computer and Communications Engineering from the American University of Beirut (AUB) in 2005, and the Ph.D. degree in Electrical and Computer Engineering from AUB in 2010. He worked as a Research Assistant in the American University of Beirut from 2004 to 2005, and in the Munich University of Technology in Spring 2005. From 2005 to 2007, he worked as a Telecommunications Engineer with Dar Al-Handasah, Shair and Partners. From November 2010 till December 2014, he worked as a Research Scientist/R&D Expert at the Qatar Mobility Innovations Center (QMIC), where he led the Broadband Wireless Access Technology Team. Afterwards, he joined Strategic Decisions Group (SDG) where he worked as a Consultant till February 2016. Then he joined the Arab Open University (AOU) as an Associate Professor and Coordinator of the M.Sc. Program in Information Security and Forensics. Between February 2018 and August 2019, he worked as an independent researcher/consultant, and he was also affiliated with AUB as a part-time faculty member. He joined Qatar University as an Associate Professor at the Computer Science and Engineering Department since August 2019. His research interests include Wireless Communications, Resource Allocation in Wireless Networks, Intercell Interference Mitigation Techniques, Antenna Theory, Sensor Networks, and Physical Layer Security.